Hopf Bifurcation Analysis in a Rotational Inverted Pendulum

D. J. PAGANO*, L. PIZARRO† and J. ARACIL‡
Departamento de Automação e Sistemas*,
Universidade Federal de Santa Catarina,
88040-900, Florianópolis,
BRAZIL.
Dpto. de Matemática Aplicada II†, Dpto. Ingeniería de Sistemas y Automática‡,
Escuela Superior de Ingenieros, Universidad de Sevilla,
Camino de los Descubrimientos s/n, 41092, Sevilla,
SPAIN.
{pagano,aracil}@cartuja.us.es; luis@matinj.us.es

Abstract: Inverted pendulums are very suitable to illustrate many ideas in automatic control of nonlinear systems. The rotational inverted pendulum is an interesting novel design that has some interesting dynamics features that are not present in inverted pendulums with linear motion of the pivot. In this paper a Hopf bifurcation, and its possible degeneracies, of the equilibrium point at the upright pendulum position that appears for the controlled closed-loop system, has been studied by means of the center manifold theorem and the normal form theory. Some numerical results are also presented in order to verify the mathematical analysis.

Key-Words: Nonlinear Control Systems, Rotational Inverted Pendulum, Bifurcations, Normal forms.

1 Introduction

Inverted pendulums have become very popular devices both as benchmark for nonlinear control analysis and for educational purposes. There are different versions of these systems. In particular, the rotational inverted pendulum developed by Furuta [1] is an interesting nonlinear complex system that allows to illustrate many different control principles.

The Furuta pendulum is basically a pole that moves freely around a pivot. This pivot can be moved through a mechanical arm connected to a DC motor. Since the acceleration of the pole can not be controlled in a direct form, the pendulum is an underactuated mechanical system. One of the control objectives is to stabilize the pole to the upper position by moving the motor arm. A linear feedback is introduced to stabilize the system at the upright unstable equilibrium position. The resulting closed-loop system has a stable local behaviour around this equilibrium. However the existence of an unstable limit cycle gives to this equilibrium its local character and makes a very difficult problem to determine the region of attraction. Nevertheless, a depth understanding of the global behaviour of the system (for instance, for the swing up problem [2]) makes imperative a detailed analysis of this unstable limit cycle, and the Hopf bifurcation associated to it.

The Furuta pendulum also has several interesting dynamic features that are not present in a pendulum with linear motion of the pivot. There is, for example, an interesting pitchfork bifurcation, for the uncontrolled system, when the pivot arm is rotated [2]. There are two equilibrium points for slow angular velocities and four equilibria at high speed. For the controlled closed-loop system there is a Hopf bifurcation of the origin that gives rise to an unstable limit cycle around this equilibrium point. This local phenomenon will be studied in this paper by means of the center manifold theorem and the normal form theory.

The equations of motion are given in Section 2. The Furuta pendulum is a four order nonlinear system that is difficult to analyze. Several approximations have been made to obtain tractable problems [1], [2]. In this paper a third order model of the Furuta pendulum is considered. This model gives a reasonable approxima-

*D. Pagano is grateful with the Brazilian Ministry of Education (CAPES) for the financial support to carry out this work under grant BEX0439/95-6. J. Aracil and Luis Pizarro have worked under project CICYT-TAP97-0553.

tion to the qualitative behaviour of the complete model system. In Section 3, normal form analysis is applied in order to provide a systematic reduction of the system representation to a minimal form (called normal form) and it is used to determine the local behaviour of the system. Some numerical results are presented in Section 4 to confirm the validity of our analysis.

2 Preliminary Results

Consider the rotational inverted pendulum as shown in Fig. 1, where θ is the angle that the pendulum (l) makes with the vertical and φ is the angle of the motor arm (r). The Furuta pendulum behaviour can

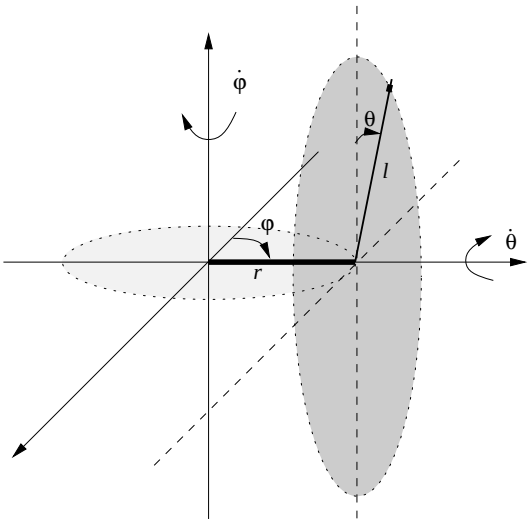

Figure 1: Furuta pendulum system, showing the motor arm and the pendulum rotational planes.

be described by the normalized equations

$$\begin{aligned} &\ddot{\theta} - \dot{\varphi}^2 \sin\theta \; cos\theta + \alpha\ddot{\varphi} \; cos\theta - \sin\theta + c_p\dot{\theta} = 0, \\ &\ddot{\varphi} + c_a\dot{\varphi} = ku, \end{aligned} \tag{1}$$

where α, k, c_p, c_a are positive constants depending on the physical pendulum characteristics; c_p, c_a are the parameters corresponding with the damping terms; and u is the control action.

Introducing $x_1 = \theta$, $x_2 = \dot{\theta}$ and $x_3 = \dot{\varphi}$, Eqs. (1) can be rewritten as

$$\begin{aligned} \dot{x}_1 &= x_2, \\ \dot{x}_2 &= \sin x_1 + x_3^2 \sin x_1 \cos x_1 \\ &\quad -\alpha(ku - c_a x_3)\cos x_1 - c_p x_2, \\ \dot{x}_3 &= ku - c_a x_3, \end{aligned} \tag{2}$$

where

$$u = l_1 x_1 + l_2 x_2 + l_3 x_3$$

is the proposed state-feedback linear control and l_1, l_2, l_3 are the control parameters. The equilibria of the system (2) are the solutions for x_1, x_2 and x_3 to the equations

$$\begin{aligned} &x_2 = 0, \\ &\sin x_1(1 + x_3^2 \cos x_1) = 0, \\ &ku - c_a x_3 = 0, \\ &u = l_1 x_1 + l_3 x_3, \end{aligned} \tag{3}$$

Therefore, solving these equations, it is found that the system has the following equilibrium points

$$\begin{aligned} &x^{e_1} = (0,0,0), \qquad x^{e_2} = \left(\pi, 0, \tfrac{k l_1 \pi}{c_a - k l_3}\right), \\ &x^{e_3} = (\bar{x}_1, 0, \bar{x}_3), \quad x^{e_4} = (2\pi - \bar{x}_1, 0, \bar{x}_3), \end{aligned}$$

where

$$\bar{x}_1 = \arccos\left[\tfrac{-(c_a - k l_3)^2}{(k l_1)^2 \bar{x}_1{}^2}\right], \bar{x}_3 = \tfrac{k l_1 \bar{x}_1}{c_a - k l_3}. \tag{4}$$

These last expressions can be graphically solved, as it is shown in Fig. 2, in order to obtain $\bar{x}_1$ and $\bar{x}_3$. Note that there exist infinite solutions to the above equations. The stability character of these equilibria

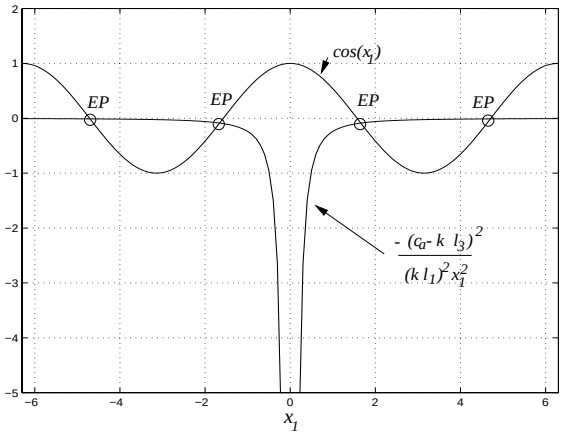

Figure 2: Graphic resolution of Eq. (4).

can be determined evaluating the Jacobian matrix at the different equilibrium points. The generic Jacobian matrix is expressed by

$$A = \begin{pmatrix} 0 & 1 & 0 \\ a_{21} & a_{22} & a_{23} \\ k\,l_1 & k\,l_2 & k\,l_3 - c_a \end{pmatrix} \tag{5}$$

where

$$\begin{aligned} a_{21} &= \cos x_1 + x_3^2 \cos^2 x_1 - x_3^2 \sin^2 x_1 \\ &\quad -\alpha\, k\, l_1 \cos x_1 + \alpha\,(k\,(l_1\, x_1 + l_2\, x_2 + l_3\, x_3) \\ &\quad -c_a\, x_3)\sin x_1, \\ a_{22} &= -\alpha\, k\, l_2 \cos x_1 - c_p, \\ a_{23} &= 2\, x_3 \sin x_1 \cos x_1 - \alpha\,(k\, l_3 - c_a)\cos x_1. \end{aligned}$$

Chosen adequately the control parameters, it is obtained that x^{e_1} is a stable equilibrium point (namely origin for the later analysis), x^{e_2} is a saddle point and the other equilibria x^{e_3}, x^{e_4} are all stable.

3 Hopf Bifurcation Analysis

In this section we study the Hopf bifurcation at the origin, and its possible degeneracies, that the system modeling the Furuta pendulum can display due to control parameter changes. Let us consider the system given by Eqs. (2). A Hopf bifurcation arises when a hyperbolic focus changes its stability, as the bifurcation parameters vary, giving rise to the appearance of small-amplitude periodic oscillations from the equilibrium state. This phenomenon is produced when a complex-conjugate pair of eigenvalues of the linearization matrix crosses the imaginary axis at certain critical parameter values. If we consider the Hopf bifurcation normal form (see [6])

$$\dot{\rho} = \alpha(\eta)\,\rho + \alpha_1\rho^3 + \alpha_2\rho^5 + \alpha_3\rho^7 + \cdots,$$

with $\alpha(0) = 0$ and η considered as the bifurcation parameter, a transversal non-degenerate Hopf bifurcation occurs when the hypothesis of a transversal crossing verifies, that is, when $\frac{d\alpha}{d\eta}(0) \neq 0$ and $\alpha_1 \neq 0$; if $\alpha_1 = 0$ and $\alpha_2 \neq 0$ a degenerate codimension 2 Hopf bifurcation, labelled DH, holds; if $\alpha_1 = \alpha_2 = 0$, $\alpha_3 \neq 0$ a degenerate codimension 3 Hopf bifurcation appears. The sign of the third-order coefficient α_1 produces two types of Hopf bifurcations: when α_1 is negative, a *supercritical* Hopf bifurcation holds (this is characterized by the stability of the periodic orbit arising from the equilibrium state); when α_1 is positive, a *subcritical* Hopf bifurcation appears (that is, an unstable periodic orbit emerges). These two cases correspond to a non-degenerate (codimension 1) Hopf bifurcation. The unfolding of the degeneracy labelled DH is characterized by the appearance, from the critical parameter values in the parameter space where the bifurcation holds, of a saddle-node of periodic orbits bifurcation locus.

Other cases of higher codimension Hopf bifurcation are possible when the higher-order coefficients in the Hopf bifurcation normal form vanish.

In order to carry out the study of the Hopf bifurcation at the origin for system (2), we consider Taylor expansions about the origin up to third-degree for the functions defining system (2), obtaining the new system

$$\begin{aligned}
\dot{x}_1 &= x_2,\\
\dot{x}_2 &= (1-\alpha k l_1)\,x_1 - (\alpha k l_2 + c_p)\,x_2\\
&\quad +\alpha\,(c_a - k l_3)\,x_3\\
&\quad +\left(\tfrac{\alpha k l_1}{2} - \tfrac{1}{6}\right)x_1^3 + x_1 x_3^2\\
&\quad +\tfrac{\alpha k}{2} l_2 x_1^2 x_2 + \tfrac{\alpha}{2}\,(k l_3 - c_a)\,x_1^2 x_3,\\
\dot{x}_3 &= k l_1 x_1 + k l_2 x_2 + k l_3 x_3 - c_a x_3.
\end{aligned} \tag{6}$$

We note that the origin is an equilibrium point for all the values of the parameters, due to the fact that the system is $\mathbf{Z}_2$-symmetric, that is, invariant under the transformation $(x, y, z) \longrightarrow (-x, -y, -z)$. To study the dynamics around the origin, we consider the linearization matrix at that equilibrium,

$$A = \begin{pmatrix} 0 & 1 & 0\\ 1-\alpha k l_1 & -\alpha k l_2 - c_p & \alpha c_a - \alpha k l_3\\ k l_1 & k l_2 & k l_3 - c_a \end{pmatrix} \tag{7}$$

whose characteristic polynomial $p(s) = s^3 - p_1 s^2 - p_2 s - p_3$ has the coefficients

$$\begin{aligned}
p_1 &= -c_p - \alpha k l_2 + k l_3 - c_a,\\
p_2 &= -c_p c_a + 1 + c_p k l_3 - \alpha k l_1,\\
p_3 &= c_a - k l_3.
\end{aligned}$$

It is easy to check that a pair of imaginary eigenvalues and a third one nonzero may arise in system (6). This degeneration occurs when $p_1 p_2 + p_3 = 0$, $p_2 < 0$, $p_3 \neq 0$. The analysis of the corresponding Hopf bifurcation at the origin will be carried out in what follows.

So, we focus on the case when the linearization matrix at the origin (7) has the eigenvalues $\lambda_{1,2} = \pm\omega_0 j$ and $\lambda_3 \neq 0$, where $\omega_0 = \sqrt{-p_2} > 0$ and $\lambda_3 = -p_3/p_2$. In this case, we have a bidimensional center manifold and a one-dimensional stable/unstable manifold, depending on the sign of λ_3.

In terms of the parameters of the linear part of the system, this degeneration occurs when:

$$l_2 = l_2^c = \frac{c_p\left(p_3^2 - p_2\right) + \alpha k l_1 p_3}{\alpha k p_2}, \quad p_2 < 0, \quad p_3 \neq 0, \tag{8}$$

or

$$l_1 = l_1^c = \frac{p_1 + p_3 - p_1 p_3 c_p}{\alpha k p_1}, \quad p_2 < 0, \quad p_3 \neq 0. \tag{9}$$

In order to know the number of periodic orbits that emerge from a Hopf bifurcation, as well as their stability, we focus on the stability analysis of the Hopf bifurcation. Considering first only codimension-one bifurcations, we can choose l_2 as bifurcation parameter. Analogous analysis can be performed using the other control parameters as bifurcation parameter. For l_2

close to the parameter value where the Hopf bifurcation takes place, l_2^c, the linearization matrix at the origin (7) has eigenvalues $\alpha(l_2) \pm j\omega(l_2)$, $\lambda(l_2)$, with

$$\alpha(l_2) = -\frac{2k\alpha^2 p_3^2 p_2^3}{4\alpha p_3^2 (p_3^2 + \omega_0^2 p_2^2)}(l_2 - l_2^c) + O\left(|l_2 - l_2^c|^2\right),$$
$$\omega(l_2) = \omega_0 + O(|l_2 - l_2^c|),$$
$$\lambda(l_2) = \lambda_3 + O(|l_2 - l_2^c|).$$

The transversality condition

$$\alpha'(l_2^c) = -\frac{2k\alpha^2 p_3^2 p_2^3}{4\alpha p_3^2 (p_3^2 + \omega_0^2 p_2^2)} \neq 0$$

holds for all the values of the parameters. Thus, all the Hopf bifurcation that may arise for system (6), both nondegenerate and degenerate, will be transversal Hopf bifurcation.

In the analysis of the stability of the Hopf bifurcation, we have to determine the first nonzero normal form coefficient for the Hopf bifurcation. To do this, first we make the linear change

$$\begin{pmatrix} x_1 \\ x_2 \\ x_3 \end{pmatrix} = \begin{pmatrix} 0 & 1 & 1 \\ \omega_0 & 0 & -\frac{p_3}{p_2} \\ \omega_0 \frac{1-p_2}{\alpha p_2} & -\frac{c_p}{\alpha} & \frac{k(l_1 p_2 - l_2 p_3)}{p_3(p_2-1)} \end{pmatrix} \begin{pmatrix} X_1 \\ X_2 \\ X_3 \end{pmatrix},$$

which yields

$$\begin{pmatrix} \dot{X}_1 \\ \dot{X}_2 \\ \dot{X}_3 \end{pmatrix} = \left(\begin{array}{cc|c} 0 & -\omega_0 & \\ \omega_0 & 0 & \\ \hline & & \lambda_3 \end{array}\right) \begin{pmatrix} X_1 \\ X_2 \\ X_3 \end{pmatrix} + \text{ N.L.T.}$$

where N.L.T. denotes nonlinear terms. Our aim is to obtain the normal form for the reduced system on the center manifold $X_3 = H(X_1, X_2)$. The quoted normal form in polar coordinates $X_1 = \rho\cos\theta$, $X_2 = \rho\sin\theta$ is

$$\dot{\rho} = \alpha_1\rho^3 + \alpha_2\rho^5 + \cdots, \quad \dot{\theta} = \omega_0 + \cdots.$$

In the study of the Hopf bifurcation of system (6) and its possible degeneracies, hand calculation (as opposed to numerical evaluation) of very long expressions is required, when the corresponding bifurcation formulae are being used. Freire *et al.* in [5] develop a recursive algorithm well suited to symbolic computation implementation, that turns out to be an efficient procedure to obtain the coefficients of the Hopf bifurcation normal form. This algorithm is based upon the use of Lie transforms; the calculations are arranged in a recursive scheme using complex variables and so the computational effort is optimized.

The application of the aforementioned algorithm, by means of a MAPLE program, allows to compute the coefficients α_1 and α_2 of order 3 and 5, respectively, of the Hopf bifurcation normal form. From the linear approximation of the center manifold, $X_3 = 0$, we get the reduced system up to third order, and we are able to obtain the first coefficient of the normal form. For the sake of brevity this coefficient is not shown in its general form in this paper. However, the expression for α_1 can be substantially reduced if it is considered the following set of system parameter values: $c_a = 0.5, c_p = 0.5, k = 41.11, \alpha = 0.42$, and the control parameter $l_3 = 1$. This set of parameter values is in agreement with the actual system. So,

$$\alpha_1 = \frac{A_1}{A_2},$$

where

$$\begin{aligned} A_1 &= -5.206\,l_2^5 + 37.437\,l_2^4 - 89.239\,l_2^3 \\ &\quad +71.776\,l_2^2 - 2.813\,l_2 - 0.144, \\ A_2 &= (0.183\,l_2^4 - 1.271\,l_2^3 + 2.929\,l_2^2 \\ &\quad -2.209\,l_2 - 0.0664)(41.11\,l_2 - 95.5). \end{aligned}$$

From $A_1 = 0$ and from Eq. (9) the pairs (l_1, l_2) corresponding to degenerate codimension-two Hopf bifurcation points can be calculated, provided that the second coefficient α_2 does not vanish. Only one solution is obtained, namely, $l_1 = 1.49, l_2 = 2.855$.

To obtain the second coefficient for the Hopf bifurcation, we need the third-order approximation to the center manifold (obtained using the method described in [4]):

$$\begin{aligned} X_3 &= -\frac{(3\,{\omega_0}^2 c_1 + 6\,{\omega_0}^2 c_3 + \lambda_3^2 c_1 + 2\,c_2\,\lambda_3\,\omega_0)\,\omega_0}{10\,{\omega_0}^2\,\lambda_3^2 + 9\,{\omega_0}^4 + \lambda_3^4} X_1^3 \\ &\quad - \frac{\lambda_3\,(3\,{\omega_0}^2 c_1 + 6\,{\omega_0}^2 c_3 + \lambda_3^2 c_1 + 2\,c_2\,\lambda_3\,\omega_0)}{10\,{\omega_0}^2\,\lambda_3^2 + 9\,{\omega_0}^4 + \lambda_3^4} X_1^2 X_2 \\ &\quad - \frac{9\,{\omega_0}^3 c_3 - 2\,\omega_0\,\lambda_3^2 c_1 + 3\,{\omega_0}^2 c_2\,\lambda_3 + 3\,\lambda_3^2\,\omega_0\,c_3 + \lambda_3^3 c_2}{10\,{\omega_0}^2\,\lambda_3^2 + 9\,{\omega_0}^4 + \lambda_3^4} X_1 X_2^2 \\ &\quad - \frac{2\,{\omega_0}^2 c_1\,\lambda_3 - 3\,{\omega_0}^3 c_2 + 7\,{\omega_0}^2 c_3\,\lambda_3 - c_2\,\lambda_3^2\,\omega_0 + c_3\,\lambda_3^3}{10\,{\omega_0}^2\,\lambda_3^2 + 9\,{\omega_0}^4 + \lambda_3^4} X_2^3, \end{aligned}$$

where

$$\begin{aligned} c_1 &= -\frac{(1-p_2)^2}{\alpha^2 p_2}, \\ c_2 &= \frac{\alpha k}{2}\omega_0 l_2^c - \frac{2c_p\omega_0(1-p_2)}{\alpha^2 p_2} - \frac{p_3\omega_0(1-p_2)}{2\alpha p_2}, \\ c_3 &= \frac{\alpha k l_1}{2} - \frac{1}{6} + \frac{p_3 c_p}{2}. \end{aligned}$$

This approximation allows to obtain the fifth-order reduced system and then we can compute the second normal form coefficient for the reduced system on the center manifold, α_2, that we do not display here due to it is rather cumbersome. Whenever $\alpha_1 = 0$ and $\alpha_2 \neq 0$, we have a Hopf bifurcation of codimension-two. We can assure that a saddle-node bifurcation of periodic orbits is present.

4 Numerical Results

In this Section numerical results obtained using AUTO software [3] are showed for the set of system parameters: $c_a = 0.5, c_p = 0.5, k = 41.11, \alpha = 0.42$. The control parameters l_1, l_2 and l_3 are selected as the bifurcation parameters. A schematic bifurcation set in the parameter plane (l_1, l_2) around a degenerate Hopf Bifurcation point (DH) is presented in Fig. 3*a*. This picture shows different system behaviour modes. Three diferent demarked frontiers: a Saddle Node Periodic Orbit, named $SNPO$, a subcritical Hopf Bifurcation, denoted by HB_{sub} and a supercritical Hopf Bifurcation, labelled as HB_{sup}, split the diagram in three different regions. In region 1 there exist only one unstable equilibrium point (saddle point); region 2 has one unstable equilibrium point at the origin and two limit cycles, the first stable and the second around it unstable; region 3 presents one stable equilibrium point and one unstable limit cycle around it. Schematic eingenvalues and state-space diagrams are also presented in Fig. 3*b*. In Fig. 4*a* it is shown the bifurcation diagram for l_1 as the bifurcation parameter. This diagram corresponds to a seccion in the plane (l_1, l_2) involving regions one and three in Fig. 3*a*. For l_1^c a subcritical Hopf Bifurcation (HB) undergoes giving rise to an unstable limit cycle. As can be seen in Fig. 4*b* the size of attraction region, delimited by this unstable limit cycle, is a function of the l_1 parameter and it is larger as l_1 increase. A Saddle-Node bifurcation of periodic orbits $(SNPO)$ occurs due to the presence of a degenerate codimension 2 Hopf bifurcation as can be observed in Fig. 5. In Fig. 6, the bifurcation and the state-space diagrams for l_2 as bifurcation parameter are shown. In Fig. 7 the bifurcation diagram for l_3 as bifurcation parameter is also shown. Note that in Fig. 7 appears a point (PB), for $l_3 = c_a/k$, where infinite equilibrium points coexist. Also, in the same figure, a Hopf bifurcation point (HB), approximately for $l_3 = 1.63$, is present. Infinite periodic orbits coexist at this singular point.

5 Conclusion

A Hopf bifurcation analysis of the equilibrium point at the upright position in the Furuta pendulum has been presented. The analysis effectuated by means of normal form theory allows to determine the different system behaviour modes when a stabilizing state-feedback controller is applied to the nonlinear model of the rotational inverted pendulum. Using these diagrams it is possible to know the range of variation of the control parameters previously to adjust the stabilizing controller. Controller robustness can be also studied applying the technique shown in this paper. Moreover, the size of the attraction region can be also

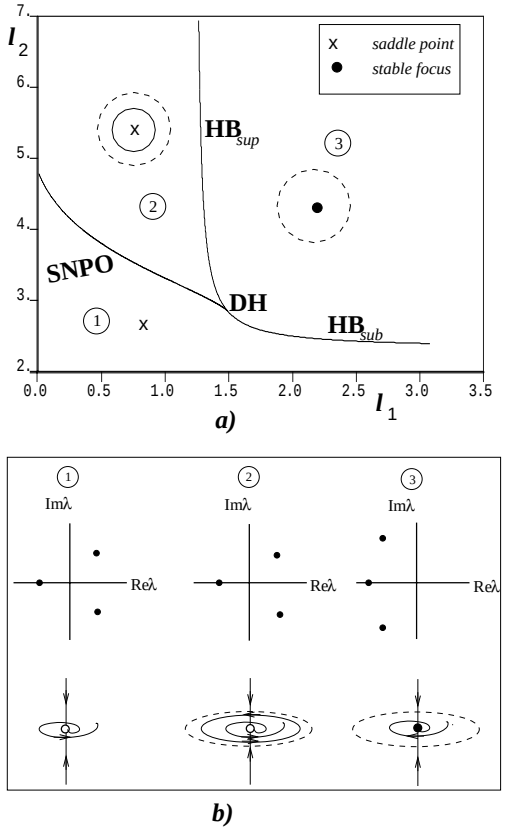

Figure 3: a) Bifurcation set around the DH point. b) Eigenvalues and state-space diagrams for the different regions shown in *a*).

estimated numerically using bifurcation diagrams constructed for the control parameters.

References

[1] K. J. Åström and K. Furuta, Swinging up a Pendulum by Energy Control. *Proceedings of the 13th IFAC World Congress*, San Francisco, USA, 1996, pp. 37-42.

[2] Aracil, J., Åström K. J. & Pagano, D. J. Global Bifurcations in the Furuta Pendulum, *Proceedings of the Nonlinear Control Systems Design Symposium (NOLCOS98)*, Vol. 1, Enschede, The Netherlands, 1998, pp. 35-40.

[3] Doedel E., AUTO 97: Continuation and Bifurcation Software for Ordinary Differential Equations. *Users Guide*, Montreal, Canada, 1997.

[4] Freire, E., Gamero E., Ponce E. and L.G. Franquelo, An Algorithm for Symbolic Computation of Center Manifolds, *Lecture Notes in Computer Science*, Vol. 358, 1989, pp. 218-230.

[5] Freire, E., Gamero E. and E. Ponce, An Algorithm for Symbolic Computation of Hopf Bifurcation, *Computers and Mathematics, E. Kaltofen and S. M. Watt (eds.), Springer-Verlag*, 1989, pp. 109-118.

[6] Guckenheimer, J. & Holmes, P., Nonlinear Oscillations, Dynamical Systems and Bifurcations of Vector Fields. (Springer-Verlag, New York). 1997.

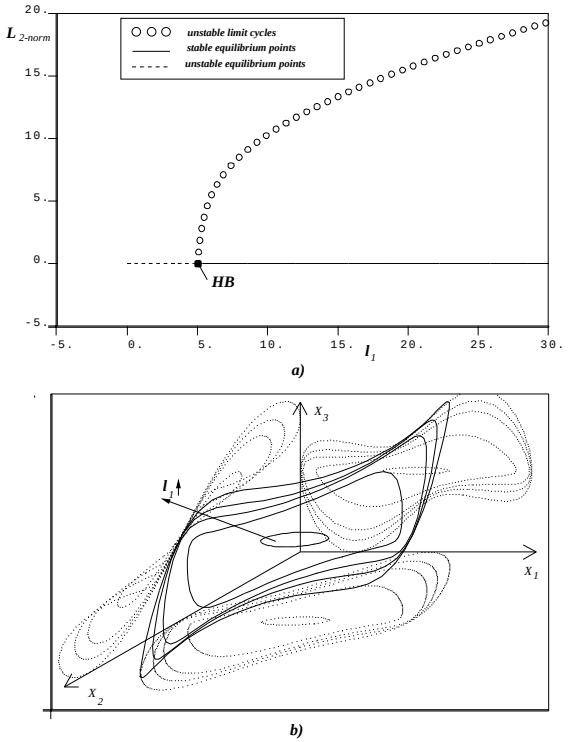

Figure 4: a) Bifurcation diagram for l_1 as the bifurcation parameter ($l_2 = 2.5$, $l_3 = 1$). b) State-space diagram showing different period orbits.

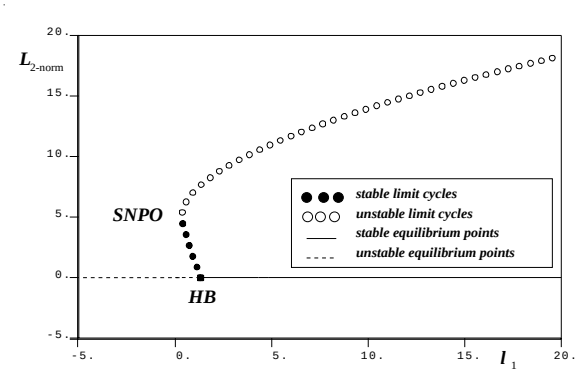

Figure 5: Bifurcation diagram for l_1 as the bifurcation parameter ($l_2 = 4$, $l_3 = 1$).

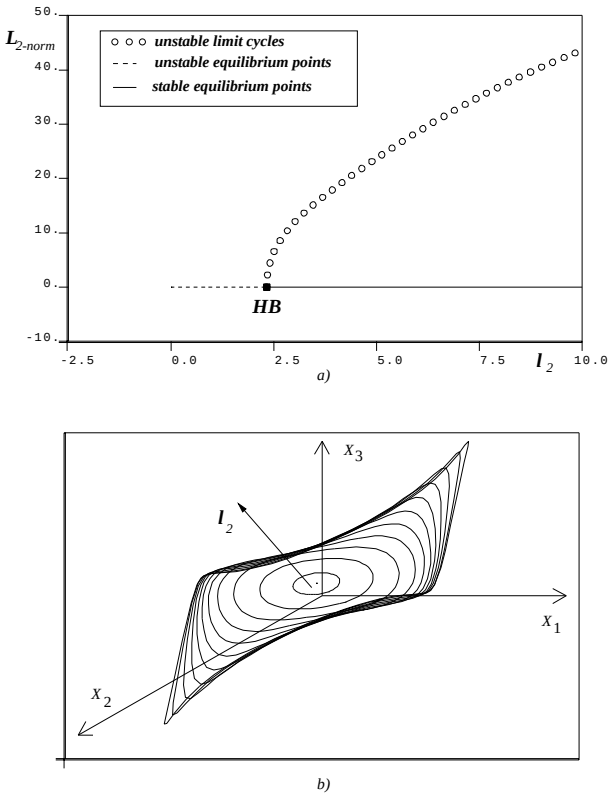

Figure 6: a) Bifurcation diagram for l_2 as the bifurcation parameter ($l_1 = 20$, $l_3 = 1$). b) State-space diagram showing different period orbits.

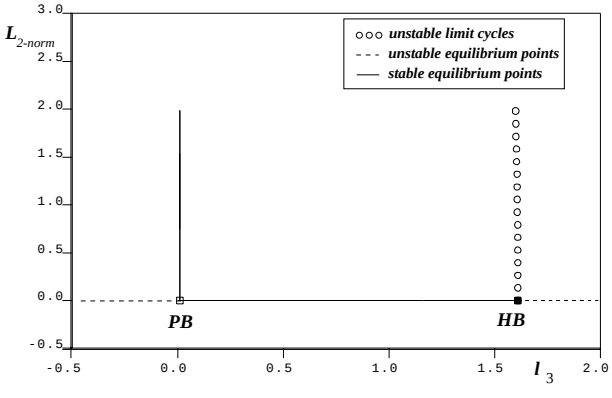

Figure 7: Bifurcation diagram for l_3 as the bifurcation parameter ($l_1 = 20$, $l_2 = 4$).